RecG interacts directly with SSB: implications for stalled replication fork regression

Jackson A. Buss[1,2], Yuji Kimura[1,2] and Piero R. Bianco[1,2,3,*]

[1]Department of Microbiology and Immunology, [2]Center for Single Molecule Biophysics and [3]Department of Biochemistry, University at Buffalo, Buffalo, NY 14214 USA

ABSTRACT

RecG and RuvAB are proposed to act at stalled DNA replication forks to facilitate replication restart. To define the roles of these proteins in fork regression, we used a combination of assays to determine whether RecG, RuvAB or both are capable of acting at a stalled fork. The results show that RecG binds to the C-terminus of single-stranded DNA binding protein (SSB) forming a stoichiometric complex of 2 RecG monomers per SSB tetramer. This binding occurs in solution and to SSB protein bound to single stranded DNA (ssDNA). The result of this binding is stabilization of the interaction of RecG with ssDNA. In contrast, RuvAB does not bind to SSB. Side-by-side analysis of the catalytic efficiency of the ATPase activity of each enzyme revealed that (−)scDNA and ssDNA are potent stimulators of the ATPase activity of RecG but not for RuvAB, whereas relaxed circular DNA is a poor cofactor for RecG but an excellent one for RuvAB. Collectively, these data suggest that the timing of repair protein access to the DNA at stalled forks is determined by the nature of the DNA available at the fork. We propose that RecG acts first, with RuvAB acting either after RecG or in a separate pathway following protein-independent fork regression.

INTRODUCTION

Genome duplication is inherently accurate, highly processive and relies on the close interplay between the genetic recombination and DNA repair machinery (1–3). Clearly, one of the main functions of recombination is to underpin faithful genome duplication. This arises due to the replication machinery frequently encountering roadblocks that have the potential to stall or collapse a replication fork (4–6). The types of lesions that could disrupt replication include proteins bound to the DNA ahead of the replication fork, noncoding lesions in the template DNA and either single- or double-strand breaks (3,7,8). Each of the different blocks could lead to a different type of damage to the DNA, and this is highlighted by the varied recombination and repair gene requirements for dealing with exposure to different types of DNA damaging agents (7–10). Whatever its source, the block has to be removed or bypassed and replication must be restarted.

In bacteria, stalled replication forks can be reversed or directly restarted (8–11). Replication fork regression can in principle be spontaneous or enzyme-driven. A spontaneous process could be driven by the positive (or negative) torsional stress ahead of replication forks that is released once the replication machinery disassembles from the DNA (12). Enzymatically, fork regression could be driven by a number of proteins (4,13–15). Over the past several years two branched DNA-specific molecular motors known as RecG and RuvAB have emerged as key players in the regression of stalled replication forks (4,16).

Genetic studies show that mutations in *recG* or either of the *ruv* genes have moderate defects in the recovery following UV irradiation or recombination when observed separately (17,18). However, when mutations in either *ruv* gene are coupled with a *recG* mutation, the resulting double mutants are severely defective (16,19). This indicates that RuvAB and RecG catalyze the same or overlapping function. Subsequent studies have shown that RecG is involved in recombinational repair pathways of both double-stranded DNA (dsDNA) breaks and single-stranded DNA (ssDNA) gaps (7,20,21). In addition to its role in recombination (19), RuvAB has also been shown to act at stalled replication forks (4). The fork repair pathways mediated by RuvAB(C) also require the function of the RecBCD nuclease/helicase. If RecBCD is absent, the forks may be cleaved, although in principle, DNA repair mechanisms that include fork regression, do not require cleavage of the DNA (4,7,22). Further work with various mutants indicates that RecG acts independently of RuvAB through a distinct pathway (2). This pathway allows for a noncleavage resolution of the DNA damage, unlike the RuvAB pathway, minimizing

*To whom correspondence should be addressed. Tel: +1 716 829 2599; Fax: +1 716 829 2158; Email: pbianco@buffalo.edu

the possibility of inappropriate recombination events (16). Thus *in vivo* data suggest that RecG and RuvAB can act synergistically or separately to facilitate genome duplication.

Biochemical analyses of both RecG and RuvAB demonstrated that each enzyme can bind to and process a variety of forked DNA substrates and recombination intermediates (23–29). RecG is a 76 kDa monomeric enzyme and is capable of acting upon a variety of 3- and 4-way junctions that are thought to mimic stalled replication forks and Holliday junctions, respectively (23,30,31). Although RecG can act during branch migration to resolve Holliday junctions, its primary role may instead be to regress or reverse stalled replication forks (2,23,32–34). In contrast, the RuvAB motor is composed of two nonidentical subunits encoded by the *ruvA* and *ruvB* genes (35). The active branch migration complex is at least 535 kDa in size and consists of a symmetric tetramer of RuvA protein which binds one face of the Holliday junction and two homo-hexameric rings of RuvB which function as chemomechanical motors to drive branch migration (36–40). The resolution complex forms when a RuvC dimer (responsible for Holliday junction cleavage at the crossover point) associates with RuvAB (28,41,42). Although RuvABC can function in replication fork processing, its primary role may instead be to perform the branch migration stage of recombination (18). Furthermore, it is clear that both enzymes can act on stalled replication fork substrates producing suitable substrates for RuvC cleavage (7,43). However, there is an important difference here as RuvAB cannot unwind forked DNA to form a Holliday Junction whereas RecG is able to do so (13,29).

Although the above-mentioned studies show that each of these proteins functions in DNA repair and has the capacity to act on model forked DNA substrates, they do not delineate how each may access a stalled replication fork resulting in its resurrection. Further, the structure of each motor complex is quite different and thus the biochemical mechanism used to process DNA substrates may also be quite different. Therefore, to more clearly understand the role of RecG and RuvAB in fork regression, we took an approach that focused on the types of DNA that might exist in the vicinity of stalled replication forks. These structures include DNA with (single-stranded DNA binding protein) SSB protein bound, DNA containing either positive or negative superhelical tension, relaxed DNA (in circular form) or linear dsDNA. We used a combination of ATPase, gel filtration and protein–protein interaction assays to determine if and how RecG or RuvAB might bind to each of these.

We found that RecG binds directly to SSB via the C-terminus of this essential protein forming a stoichiometric complex of 2 RecG monomers per SSB tetramer. Binding to SSB occurs in solution and on ssDNA resulting in stabilization of the binding of RecG to ssDNA. In contrast, we did not detect any interaction between SSB and either RuvA, RuvB or the RuvAB complex. Next, we extended our ATPase analysis of RecG (44) and that of RuvAB by the Cox group (45). We compared the ability of each protein to efficiently hydrolyze ATP in

the presence of six different DNA cofactors, relevant to the role of each protein at a stalled fork. The results show that (−)scDNA and ssDNA are the optimal cofactors for RecG and the only cofactor for which RuvAB showed a preference relative to RecG was relaxed circular DNA.

Collectively, these data provide insight into the timing of repair protein access to the DNA at a stalled replication forks. We propose that at early times following stalling of the replication machinery, if the DNA is (−)supercoiled, RecG is favored to act. Similarly, if the DNA has exposed single stranded regions, these would be bound by SSB, and again RecG would be directed onto the DNA in preference over RuvAB. Only at later times once the DNA has been relaxed and/or a Holliday junction-like structure has been produced, would RuvAB be favored to act. A model is provided to explain the sequential and separate actions of RecG and RuvAB in fork regression.

MATERIALS AND METHODS

Chemicals

Phosphoenol pyruvate (PEP), nicotinamide adenine dinucleotide (NADH), pyruvate kinase (PK), lactate dehydrogenase (LDH) and the ssDNA-cellulose resin were from Sigma. ATP, DEAE Sepharose Fast Flow, Q-Sepharose, the 16/10 heparin FF and the Mono S 5/50 GL columns were from Amersham. Phosphocellulose (P11) was from Whatman. Bio-Gel® HTP hydroxylapatite was from Bio-Rad. Dithiothreitol (DTT) was from Acros Organics. BSA and HindIII were purchased from New England Biolabs. Wheat Germ Topoisomerase I (WGT) was from Promega.

Reagents

All solutions were prepared using Barnstead Nanopure water. Stock solutions of PEP were prepared in 0.5 M Tris–acetate (pH 7.5). ATP was dissolved as a concentrated stock in 0.5 M Tris–HCl (pH 7.5), with the concentration determined spectrophotometrically using an extinction coefficient of $1.54 \times 10^5 \, \text{M}^{-1} \, \text{cm}^{-1}$. NADH was dissolved in 10 mM Tris–acetate (pH 7.5), concentration determined using an extinction coefficient of $6250 \, \text{M}^{-1} \, \text{cm}^{-1}$, and stored in small aliquots at −80°C. DTT was dissolved as a 1 M stock in nanopure water and stored at −80°C. All reaction buffers described below were assembled at 10 times reaction concentration and stored in 1 ml aliquots at −80°C.

DNA cofactors

For all DNA cofactors, the concentrations of stock solutions were determined in micromolar nucleotides using the extinction coefficients as indicated below. To permit direct comparisons between DNA cofactors, concentrations and subsequent $k_{\text{m}}^{\text{DNA, app}}$ values are reported in nanomolar, (nM) molecules for all assays.

Negatively scDNA (pPB67) was purified using two different procedures as described previously (44). The first method utilized alkaline lysis followed by two successive isopycnic centrifugations in CsCl gradients (46). This preparation was designated (−)scDNA#1.

The second method designated (−)scDNA#2, involves triton lysis followed by 2 successive CsCl gradients and a sucrose gradient in high salt (47). For all preparations of dsDNA, the concentration was determined spectrophotometrically using an extinction coefficient of $6500\,M^{-1}\,cm^{-1}$.

Linear dsDNA was produced by subjecting (−)scDNA#1 to cleavage by HindIII. Following heat inactivation, the sample was extracted with an equal volume of phenol:chloroform:iso-amyl alcohol (PCI; 25:24:1) followed by an equal volume of TE-saturated ether. The DNA was subsequently ethanol precipitated, dried, resuspended in $1\times$ TE buffer (pH 8.0) and concentration determined.

Relaxed circular DNA was prepared by treating (−)scDNA#1 with WGT. Reactions ($200\,\mu l$) contained $25\,\mu g$ of (−)scDNA and 100 U of WGT in a buffer of 50 mM Tris–HCl (pH 7.5), 50 mM NaCl, 0.1 mM EDTA, 1 mM DTT and 20% (v/v) glycerol. After incubation at 37°C for 60 min, the enzyme was removed by PCI and ether extractions. Following ethanol precipitation and concentration determination, agarose gel electrophoresis was used to confirm conversion of (−)scDNA to the relaxed form.

M13 mp18 ssDNA was prepared as described (44). The concentration of DNA was determined spectrophotometrically using an extinction coefficient of $8,780\,M^{-1}\,cm^{-1}$ (nucleotides). Purified DNA was stored in small aliquots at −80°C.

Positively supercoiled pBR322 DNA was purchased from John Innes Enterprises (Norwich, UK). It was produced by treating relaxed circular pBR322 DNA with an excess of DNA gyrase.

Proteins

RecG protein was purified as described previously (44), with the following modifications: the first column was a 30 ml Q-Sepharose column equilibrated in Buffer A [20 mM Tris–HCl (pH 8.5), 1 mM EDTA, 1 mM DTT, 10 mM NaCl]. The protein was eluted using a linear gradient (10–1000 mM NaCl) with RecG eluting between 250 and 360 mM NaCl. The pooled fractions were subjected to heparin FF and hydroxylapatite chromatography as described (44). Pooled fractions from the hydroxylapatite column were dialyzed overnight into S Buffer [10 mM KPO_4 (pH 6.8), 1 mM DTT, 1 mM EDTA and 100 mM KCl]. The protein was applied to a 1 ml MonoS column and eluted using a linear KCl gradient (100–700 mM) with RecG eluting at 350 mM KCl. The fractions containing RecG were pooled and dialyzed overnight against storage buffer [20 mM Tris–HCl (pH 7.5), 1 mM EDTA, 1 mM DTT, 100 mM NaCl and 50% (v/v) glycerol]. The protein concentration was determined spectrophotometrically using an extinction coefficient of $49\,500\,M^{-1}\,cm^{-1}$ (48). The modifications to the purification procedure yielded a 4-fold increase in specific activity relative to that used previously (44).

RuvA and *RuvB* proteins were purified as described previously (45). The concentration of RuvA was determined using the extinction coefficient of $5550\,M^{-1}\,cm^{-1}$ (49).

For the RuvB purification, the DEAE Biogel A column was replaced by a 100 ml Q-Sepharose column that was equilibrated with TEGD buffer [20 mM Tris–acetate, 1 mM EDTA, 10% (v/v) Glycerol and 1 mM DTT] and the protein eluted with a 1 l linear gradient from 0 to 500 mM potassium acetate. The concentration of RuvB protein was determined using the extinction coefficient of $16\,400\,M^{-1}\,cm^{-1}$ (49).

SSB proteins—*Escherichia coli* single stranded DNA-binding protein (SSB) was purified from strain K12ΔH1Δtrp as described (50). The concentration of purified SSB protein was determined at 280 nm using $\varepsilon = 30\,000\,M^{-1}\,cm^{-1}$. The site size of SSB protein was determined to be 10 nucleotides per monomer by monitoring the quenching of the intrinsic fluorescence of SSB that occurs on binding to ssDNA, as described (51). The SSB113 and SSBΔC8 mutant proteins were provided by Dr James Keck, University of Wisconsin-Madison. Bacteriophage gene 32 protein (gp32) was purified as described (52). The concentration of purified gp32 was determined at 280 nm using $\varepsilon = 37\,000\,M^{-1}\,cm^{-1}$ (53). The site size of gp32 was determined to be 7 nucleotides/monomer by monitoring the quenching of the intrinsic fluorescence of gp32 that occurs on binding to ssDNA, as described (51).

ATP hydrolysis assay

The hydrolysis of ATP was monitored using a coupled spectrophotometric assay (44). The standard reaction buffer for RecG contained 20 mM Tris–acetate (pH 7.5), 1 mM DTT, 0.3 mM NADH, 7.5 mM PEP, 20 U/ml PK, 20 U/ml LDH, 100 nM RecG, 1 mM ATP and 10 mM magnesium acetate (but varied according to the DNA cofactor present). The reaction buffer for RuvAB was the same as for RecG, except RecG was replaced by RuvAB and 2 mM DTT, 100 μg/ml BSA and 6.3% (w/v) glycerol were used (45). Assays were performed in a reaction volume of 150 μl, and were initiated by the addition of enzyme following a 2 min preincubation of all other components. The concentrations of RuvA and RuvB were held constant at 1.3 μM and 1 μM, respectively (2 RuvA tetramers:1 RuvB-hexamer), and were mixed together for 30 min on ice prior to addition (45). Using these concentrations the concentration of RuvAB complex was calculated to be 167 nM. The rate of ATP hydrolysis was calculated by multiplying the slope of a tangent drawn to linear portions of time courses by 159. In a typical reaction, close to 200 data points were used to draw a linear fit to the data to calculate reaction rates.

In salt-titration experiments, the same RecG or RuvAB reaction buffers were used. The concentration of M13 ssDNA was 36 μM nucleotides, SSB proteins (either wild-type or mutant) were present at 1.8 μM, RecG was at 100 nM and RuvAB at 167 nM complex. Reactions were initiated by the addition of either RecG or RuvAB following a 5 min incubation of all other components. Once a steady state rate of ATP hydrolysis was achieved, NaCl was added in 12.5 mM increments (1 μl volumes). This was repeated until all ATP hydrolysis of RecG ceased. The resulting hydrolysis rate in each steady state region

was calculated and expressed as a percent of the steady state rate in the absence of NaCl. The total volume used to calculate final concentration of NaCl was adjusted after each addition in order to correct for the additions themselves. A line of best fit was drawn for data points between each addition to obtain the ATP hydrolysis rate after each salt increment. The average number of data points used to determine the reaction rate was 14. These rates were subsequently graphed to determine the concentration of NaCl resulting in a 50% reduction in the rate of ATP hydrolysis which corresponds to the salt-titration midpoint.

Coprecipitation

Coprecipitation of SSB or T4 gp32 and either RecG, RuvB or RuvAB, was done using a method described for SSB and RecQ (54). Reactions were done on ice in a volume of 20 μl and contained 20 mM Tris–HCl (pH 7.5), 150 mM NaCl, 10% glycerol, 1 mM DTT, 24.9 μM SSB monomers (or 19.8 μM gp32 in place of SSB). Where present, RecG, RuvB or RuvAB (ratio of 1.3 : 1; A : B) were added to a final concentration of 20 μM. Following mixing, tubes were incubated on ice for 15 min, mixed with an equal volume of ammonium sulfate precipitation buffer [reaction buffer plus 2.6 M NH$_4$(SO$_4$)] and incubated for an additional 15 min. The mix was subjected to centrifugation at 21 000×g at 4°C for 1 min. The supernatant was removed to a fresh tube and the pellet was then washed three times with 40 μl of precipitation buffer with each wash followed by an identical centrifugation run. The final pellet was resuspended into 40 μl of 1× reaction buffer. Thereafter, 20 μl of the pellet or supernatant fraction were mixed with an equal volume of 2× SDS–PAGE loading buffer, boiled for 2 min and 20 μl of each sample subjected to electrophoresis in 12% SDS–PAGE gels. Following electrophoresis, gels were stained with Coomassie brilliant blue, destained and photographed. Quantitation of all gels was done using Image Quant Software (v5.0, GE Biosciences).

Gel filtration

To detect complex formation, samples (500 μl; assembled in ATPase assay buffer with the optimal Mg^{2+} for each protein) were applied to a Superose 6 column (GE Biosciences) equilibrated in buffer containing 20 mM Tris–HCl (pH7.5), 1 mM DTT, 5 mM Mg(OAc)$_2$ and 150 mM NaCl. The column was connected to a Biologic Duoflow Chromatography system (Bio-Rad Laboratories). Following chromatography, fractions were subjected to electrophoresis on 12% SDS–PAGE gels to evaluate fraction composition. Gels were stained using Coomassie brilliant blue (Bio-Rad) or silver (SilverSnap II; PIERCE).

The following samples were applied to the column: DNA only (400 μM nucleotides); each protein alone (5 μM for RecG, RuvA or RuvB; 20 μM for SSB); each protein in the presence of M13 ssDNA and, in separate runs RecG, RuvA or RuvB (5–50 μM of each in separate runs) were added to preformed, stoichiometric complexes of M13 ssDNA and SSB. To test for species-specific interactions, SSB was replaced by gp32 (used at 20 μM) and

RecG was added following complex formation. All binding experiments were done at 0°C; SSB (or gp32) was added to buffer containing ssDNA for 10 min followed by either RecG, RuvA or RuvB and an additional 30 min incubation.

RESULTS

The C-terminus of SSB is required to stabilize the RecG-ssDNA interaction

The C-terminal 60 residues of SSB end in a highly conserved sequence (Met-Asp-Phe-Asp-Asp-Asp-Ile-Pro-Phe) which is disordered in the crystal structure of the protein bound to DNA (55). As this region extends from the structure of SSB bound to DNA, it was proposed to be involved in mediating SSB-protein interactions with components of the replisome. It was later shown that not only did SSB bind to components of the replisome but to other repair proteins as well including PriA, RecQ and Topoisomerase III (54,56–60). Not surprisingly, mutations within the conserved sequence either reduce or eliminate binding of SSB to these proteins.

Previously, we demonstrated using the salt-titration midpoint (STMP) of the ATPase activity of RecG, that wild-type SSB protein stabilizes the interaction of RecG with ssDNA producing a 2-fold increase in the STMP (44). To determine whether the stabilization of RecG is mediated via the C-terminus of SSB, we evaluated the effects of the SSB113 or SSBΔC8 proteins on the STMP and compared them to wild-type. SSB113 has a point mutation in the penultimate residue of the conserved sequence, while SSBΔC8 has the last eight residues deleted. Thus if the C-terminus is required for stabilization, these mutants are expected to reduce (SSB113) or eliminate (SSBΔC8) the increase in the STMP of RecG.

The results show that the STMP for RecG in the presence of ssDNA is 35 mM (Figure 1). The addition of wild-type SSB protein results in a 2-fold increase in the STMP to 67 mM, consistent with previous results (44). The presence of SSB113 also results in an increase in the STMP but only 1.3-fold to 45 mM. In contrast, the presence of SSBΔC8 results in a 2.7-fold decrease in the STMP relative to wild-type, down from 67 mM to 25 mM. In other words, loss of the last eight residues of SSB produces a protein which destabilizes the binding of RecG on ssDNA. These results demonstrate that the C-terminus of SSB is necessary to stabilize the binding of RecG to ssDNA.

Similar salt-titration experiments were done with RuvAB. However, no effect of either wild-type or mutant SSB proteins was observed on the STMP of the ATPase activity of RuvAB (data not shown).

RecG binds directly to SSB protein via the C-terminus

The stabilization of RecG afforded by SSB could be mediated directly via protein–protein interactions or alternatively, indirectly via the DNA. To test for direct interactions, we used an ammonium sulfate coprecipitation technique. This approach has been successfully used in previous studies to demonstrate separate,
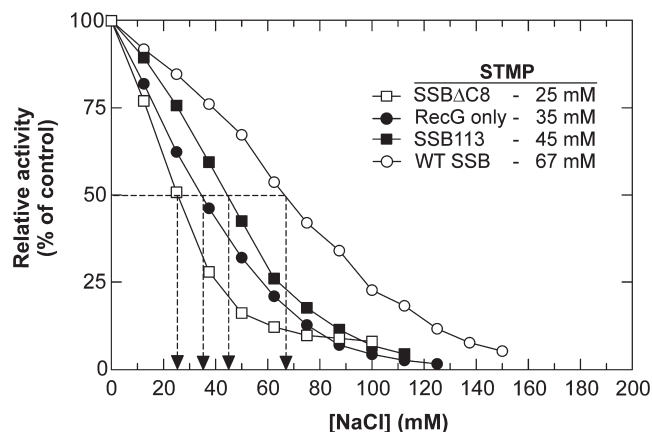
Figure 1. Stabilization of RecG on ssDNA by SSB requires the C-terminus of SSB. Reactions were conducted as described in Materials and methods section. To obtain the STMP the resulting rates of ATP hydrolysis at each concentration of NaCl were calculated during each phase of the assay following addition of NaCl, and expressed as a percent of the reaction rate in the absence of added NaCl. The dashed lines indicate the STMP for each reaction. Only a single salt titration is shown for each reaction condition. The error from independent experiments is ±3 mM. (Filled circle), RecG only; (open circle), RecG + wild-type SSB; (open square), RecG + SSBΔC8 and (filled square), RecG + SSB113.

DNA-independent interactions between Exonuclease I, RecQ and TopoIII with SSB (54,56,60). This technique works well because neither Topoisomerase III, Exonuclease I nor RecQ precipitates efficiently at the low concentration of ammonium sulfate used when SSB is absent.

To determine whether RecG interacts with SSB, coprecipitation experiments were done and the results are presented in Figure 2. SSB precipitates effectively as expected (Figure 2A). The addition of RecG results in efficient coprecipitation with ~75% of the input RecG remaining in the pellet. Importantly, only 12% of the input RecG precipitated in the absence of SSB (Figure 2B). To show that the coprecipitation was specific to SSB, we replaced SSB with T4 gene 32 protein. In contrast to the SSB reaction, only 16% of the RecG was found in the pellets with gp32 (Figure 2B). Thus RecG binds directly and specifically to SSB.

The C-terminus of SSB is necessary for the stabilization of the ATPase activity of RecG on ssDNA (Figure 1). Previous work with RecQ and PriA has shown that these proteins interact with SSB directly via the SSB C-terminus (54,56). To determine whether the C-terminus of SSB is also required for binding to RecG, coprecipitation reactions were repeated using in parallel, SSB, SSB113 and the SSBΔC8 proteins. The analysis of three separate assays for each protein is shown in Figure 2C. The results show that 74% of the input RecG coprecipitated with wild-type SSB. This value decreased 1.7-fold to 44% when wild-type was replaced by SSB113 and 3-fold to 24% when SSBΔC8 was used instead. The amount of RecG coprecipitated in the presence of SSBΔC8 is only marginally higher than that observed in the presence of gp32 or when only RecG is present. Therefore, and as

observed previously for PriA, RecQ and TopoIII, the physical interaction between RecG and SSB is mediated via the C-terminus of SSB protein.

To further characterize the interaction between RecG and SSB, a titration of RecG was done followed by protein coprecipitation and analysis of the resulting Coomassie-stained, SDS–PAGE gels. In these experiments, the concentration of SSB was held constant at 5 μM tetramer and the concentration of RecG was varied from 1 to 23 μM. Analysis of the resulting gels reveals a solution stoichiometry of 2 RecG monomers per SSB tetramer (Figure 2D).

RuvA, RuvB and RuvAB do not bind to SSB

As RuvAB has been proposed to be involved in replication fork reversal, these proteins were tested for their potential interaction with SSB as well. RuvA and B were tested separately and also as a preformed RuvAB complex. The results show that 30% of the input RuvB coprecipitated with SSB whereas we did not detect any RuvA in the pellet fractions with SSB (Figure 2A). In contrast to RecG, RuvB precipitated in the absence of SSB with 30% of the input protein being found in the pellet fraction (Figure 2B). Similar levels of RuvB were detected in pellet fractions when equivalent amounts of preformed RuvAB complexes were used instead of RuvB alone (Figure 2B). Under these conditions, 30% of the RuvA coprecipitated as well (data not shown). This coprecipitation is not due to a novel RuvAB interaction revealed when RuvB is present but instead results from the RuvA–RuvB interaction and RuvB precipitation independent of an interaction with SSB.

As RuvB is able to precipitate independently of SSB, it is conceivable that the standard conditions may mask the potential interaction between these proteins. Therefore, we decreased the concentration of ammonium sulfate in 50% increments in an attempt to find a concentration where RuvB would no longer precipitate on its own. Using this concentration (i.e. 0.85 M ammonium sulfate), increasing amounts of RuvB were added to fixed concentrations of SSB and coprecipitated. The results show that at the concentrations tested, RuvB did not efficiently coprecipitate with SSB (Figure 3A and C) and even at higher concentration of RuvB, efficient SSB-independent precipitation was not observed (data not shown). Identical experiments were done with RecG and as we observed using standard conditions, efficient precipitation of RecG was observed at concentrations ⩾5 μM (Figure 3B and C). A small amount of RecG did coprecipitate even at the lowest concentration of RecG tested. Under these suboptimal ammonium sulfate conditions, the stoichiometry of 2 RecG monomers per SSB tetramer was maintained (data not shown).

SSB and RecG co-exist on ssDNA

To further analyze the interaction between RecG or RuvB and SSB, we used native gel filtration to evaluate the interactions in the presence of ssDNA. This technique was used to determine whether complexes of either SSB and RecG or RuvB and SSB could be detected on ssDNA
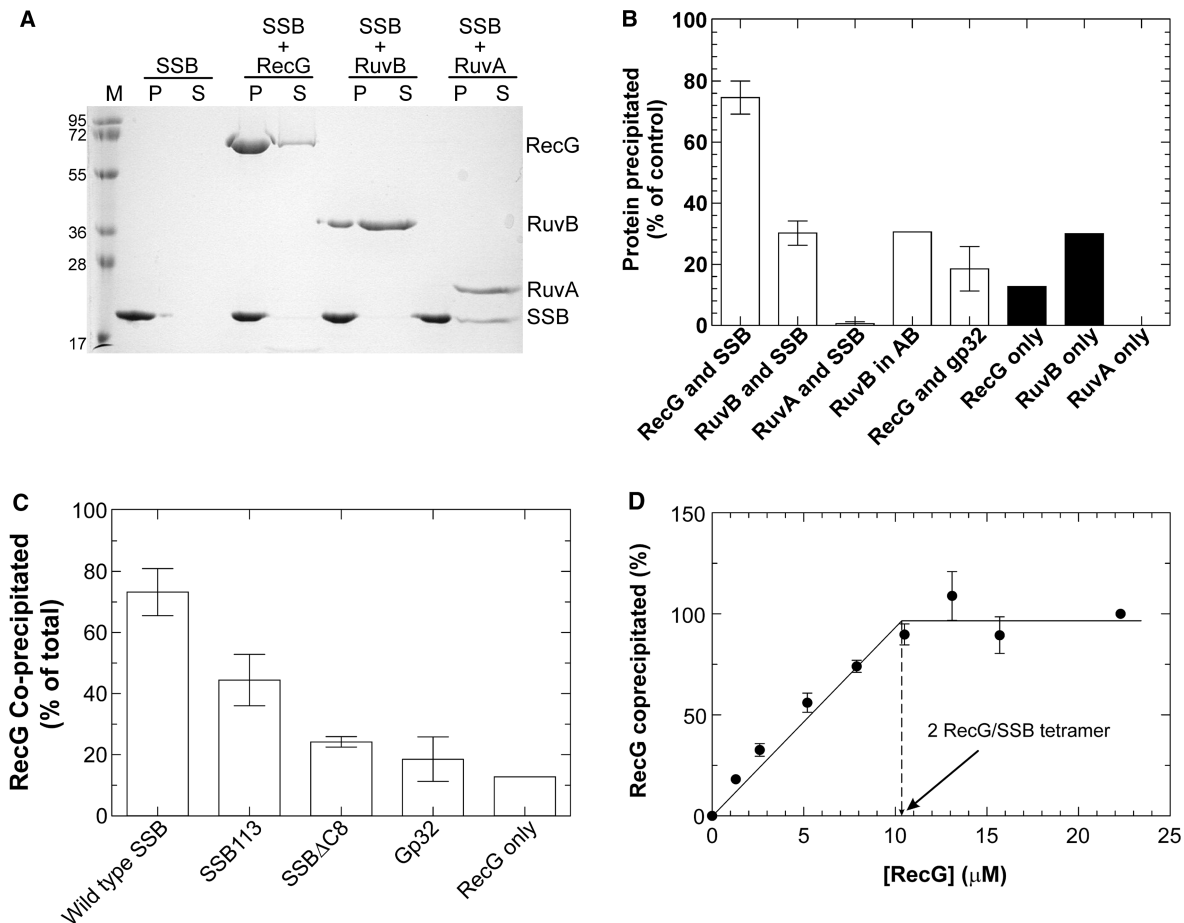
Figure 2. RecG interacts with the C-terminus of SSB protein. (**A**) A Coomassie-stained SDS–PAGE gel of coprecipitation assays. P, pellet; S, supernatant fractions following precipitation. The identity of each protein is indicated to the right of the gel. M, molecular weight marker. (**B**) Analysis of several coprecipitation gels. Error bars indicate the error from 3 to 5 independent experiments. The amount of protein present in each pellet is expressed as a fraction of the total amount added to coprecipitation experiments. This amount of protein was loaded onto gels in the adjacent lanes to permit equivalent staining and precise quantitation. (**C**) Analysis of gels such as that shown in (A) where coprecipitation of RecG was assayed in the presence of different SSB proteins as indicated. The amount of RecG present in pellet fractions is expressed as a fraction of the total present in the pellet and supernatant fractions. (**D**) RecG forms a stoichiometric complex with SSB. The analysis of 3 RecG titrations is shown. In each assay, 5 μM SSB was used and proteins were precipitated as described in Materials and methods section. The amount of RecG present in each pellet is expressed as a fraction of the total amount added to coprecipitation experiments, i.e. the total amount present in pellet and supernatant fractions as determined by analysis of Coomassie-stained SDS–PAGE gels. The amount of RecG precipitated in each titration was normalized to the maximum amount precipitated in the titration to permit comparison between assays.

simultaneously. Here, stoichiometric complexes of SSB and M13 ssDNA were preformed and then in separate reactions, either RecG or RuvB was added. The resulting mixtures were subjected to gel filtration followed by SDS–PAGE analysis to detect for the presence of each protein. These results are presented in Figure 4 and summarized in Table 1. We used only M13 ssDNA in these experiments to look for specific SSB-protein interactions. Forked substrates with dsDNA regions were not used so that binding by test proteins to duplex DNA would be eliminated.

First, separate control gel filtration runs were done to ascertain the elution positions of M13 ssDNA and each of the proteins in the absence of DNA (Table 1). Second, SSB was bound to ssDNA and subjected to gel filtration. This resulted in a small shift in the apex of the ssDNA peak from 7.5 to 7.1 ml. SDS–PAGE analysis showed that as expected, the shift in position of the first peak was due
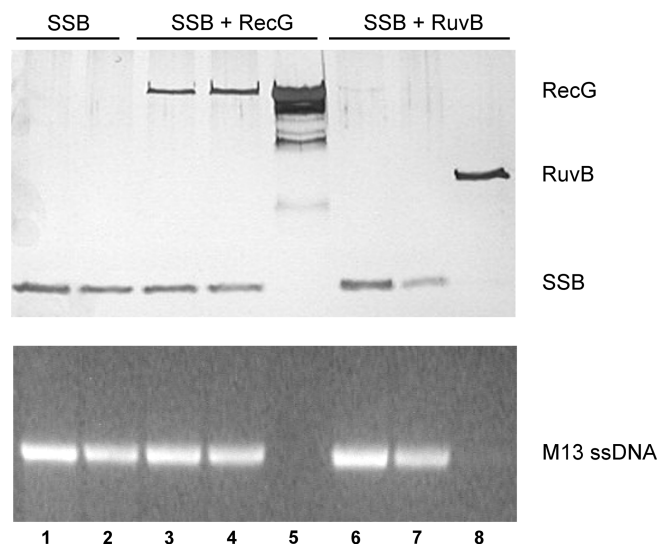
to the presence of SSB binding to the DNA (Figure 4, lanes 1 and 2). As an excess of SSB was used in this experiment, a second peak eluted later from the column at the position corresponding to free protein (Table 1 and data not shown). Next, a stoichiometric SSB–ssDNA complex was formed, RecG was added and allowed to bind. The resulting gel filtration profile showed a peak that eluted at 6.5 ml and a second peak eluting at 16.5 ml. The latter peak contained free RecG only while the former contained M13 ssDNA, SSB and RecG (Figure 4 and Table 1). Quantitation of the amounts of SSB and RecG present in the peak fractions corresponding to the protein–DNA complex (Figure 4, lanes 3 and 4) yielded a stoichiometry of 1 RecG per SSB monomer.

To evaluate RuvB binding, the SSB–DNA complex was formed as before and RuvB added and allowed to bind for 30 min. The subsequent gel filtration profile showed two
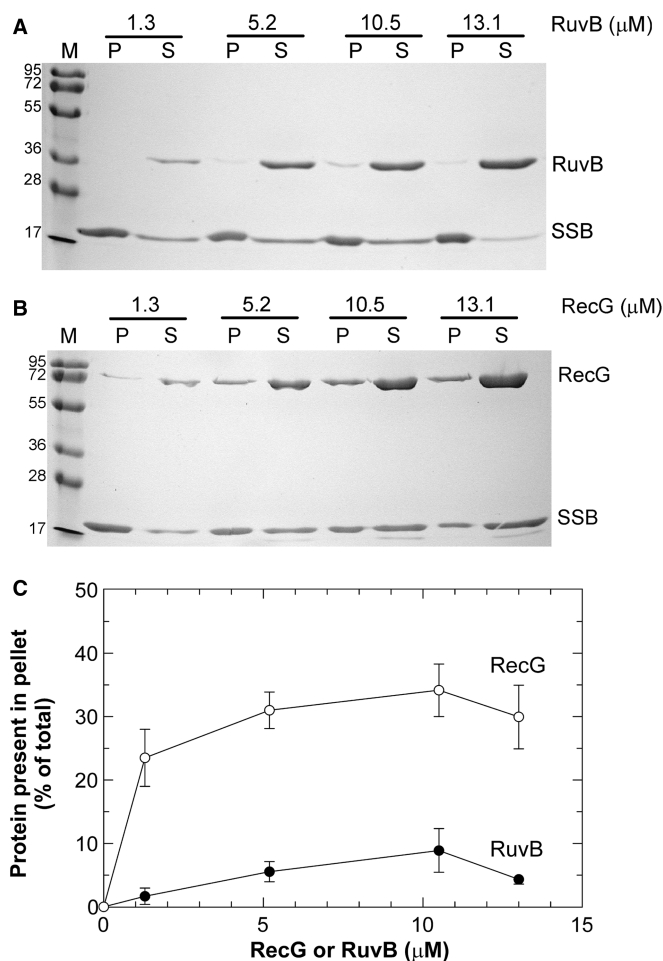
Figure 3. RecG and not RuvB forms a stoichiometric complex with SSB. (**A**) A Coomassie-stained SDS–PAGE gel of coprecipitation assays with RuvB and SSB. (**B**) A Coomassie-stained SDS–PAGE gel of coprecipitation assays with RecG and SSB. The concentration of ammonium sulfate used in panels A and B was 0.85 M. The reactions are otherwise identical to those in Figure 2. M, molecular weight marker; P, pellet; S, supernatant fractions. (**C**) Quantitation of protein coprecipitation assays. The analysis is of three separate assays for each protein done using 0.85 M ammonium sulfate and includes the gels shown in panels A and B. The amount of protein precipitated is expressed as a fraction of the total amount detected in the P and S lanes of each reaction.

Figure 4. RecG and SSB form a stable complex on ssDNA. Gel analysis of relevant fractions from gel filtration elution profiles is shown. Complexes were formed on ice for 30 min prior to subjecting them to gel filtration. Immediately before loading, the salt concentration was adjusted to 150 mM to match that of the column running buffer. The reactions shown contained binding buffer as indicated in Materials and methods section and 200 µM M13 ssDNA, 20 µM SSB and either 20 µM RecG or RuvB. Top panel, a silver-stained SDS–PAGE gel; bottom panel an agarose gel stained with ethidium bromide. For each fraction, identical volumes were loaded onto each gel. The relevant bands are indicated to the right of each gel. The position of migration of each protein band was determined relative to molecular weight markers and for M13 ssDNA, a combination of DNA ladder and M13 ssDNA was used (not shown). Lanes 1 and 2, fractions from the SSB-DNA peak; lanes 3 and 4, the RecG-SSB-ssDNA peak; lane 5, free RecG which eluted from the column at a later time; lanes 6 and 7, the putative SSB-RuvB-ssDNA peak and lane 8, free RuvB which eluted later than the SSB-DNA peak. The small amount of more slowly migrating species in lane 6 of the SDS–PAGE gel is the result of a small amount of RecG from lane 5.

peaks similar to that observed for RecG-SSB. However and in contrast to RecG, the first peak eluting at 7.1 ml contained only SSB and no detectable levels of RuvB (Figure 4, lanes 6 and 7 and Table 1) while the second peak eluting at 15 ml contained only RuvB (Figure 4, lane 8 and Table 1). Finally, to determine whether the co-complex of DNA, SSB and RecG was specific, binding was repeated where SSB was replaced with T4 gp32. The resulting profile showed two peaks with only gp32 in the first peak with ssDNA and no RecG which was present in the second peak (Table 1). Therefore, and consistent with the STMP and coprecipitation data, SSB and RecG form a specific complex that exists both in solution and when bound to ssDNA. Further, we did not detect complex formation between RuvB and SSB.

ssDNA is a poor cofactor for the ATPase activity of RuvAB

The above-mentioned experiments suggest that RecG acts on stalled replication forks when the ssDNA in the fork is bound by SSB. Further, these data also suggest that these forks with single-stranded character should not be bound by RuvAB. However, this is only one possible DNA–protein structure that may result from replisome stalling and/or disassembly. To begin to understand how RecG or RuvAB might access the DNA at a stalled replication fork, we performed a side-by-side analysis of the ATPase activity of each protein on six separate DNA substrates.

Previous work has characterized the ATPase activity of each protein on a variety of DNA substrates (44,45,49). The experiments described below extend previous work and compare the activity of each protein on the same preparations of DNA and in all cases, experiments with each enzyme were done on the same day. In instances where a DNA preparation was depleted, experiments were repeated with the new preparation for each enzyme. Further, for each enzyme in separate experiments, a magnesium titration was done to determine the

optimal magnesium to ATP ratio to use in all experiments [data not shown and (44,45,49)]. To ensure that ATP was not rate limiting, it was present at concentrations well above the K_m or $S_{0.5}$, depending on the DNA cofactor present.

First, and to complete the study of ssDNA, a DNA titration was done using M13 ssDNA and the rates of the two proteins compared. Of the DNA cofactors used in this study, ssDNA is the poorest for RuvAB producing a k_{cat} of $383 \pm 12 \, \text{min}^{-1}$ and correspondingly low catalytic efficiency of only $129 \, \text{min}^{-1} \text{nM}^{-1}$ (Table 2). In contrast, the k_{cat} for RecG in the presence of ssDNA is 3.1-fold higher than that of RuvAB ($1180 \pm 28 \, \text{min}^{-1}$) and, more importantly, the catalytic efficiency is 11-fold higher than that of RuvAB. The elevated level of activity of RecG

relative to RuvAB on ssDNA is in agreement with the STMP, coprecipitation and gel filtration data presented above.
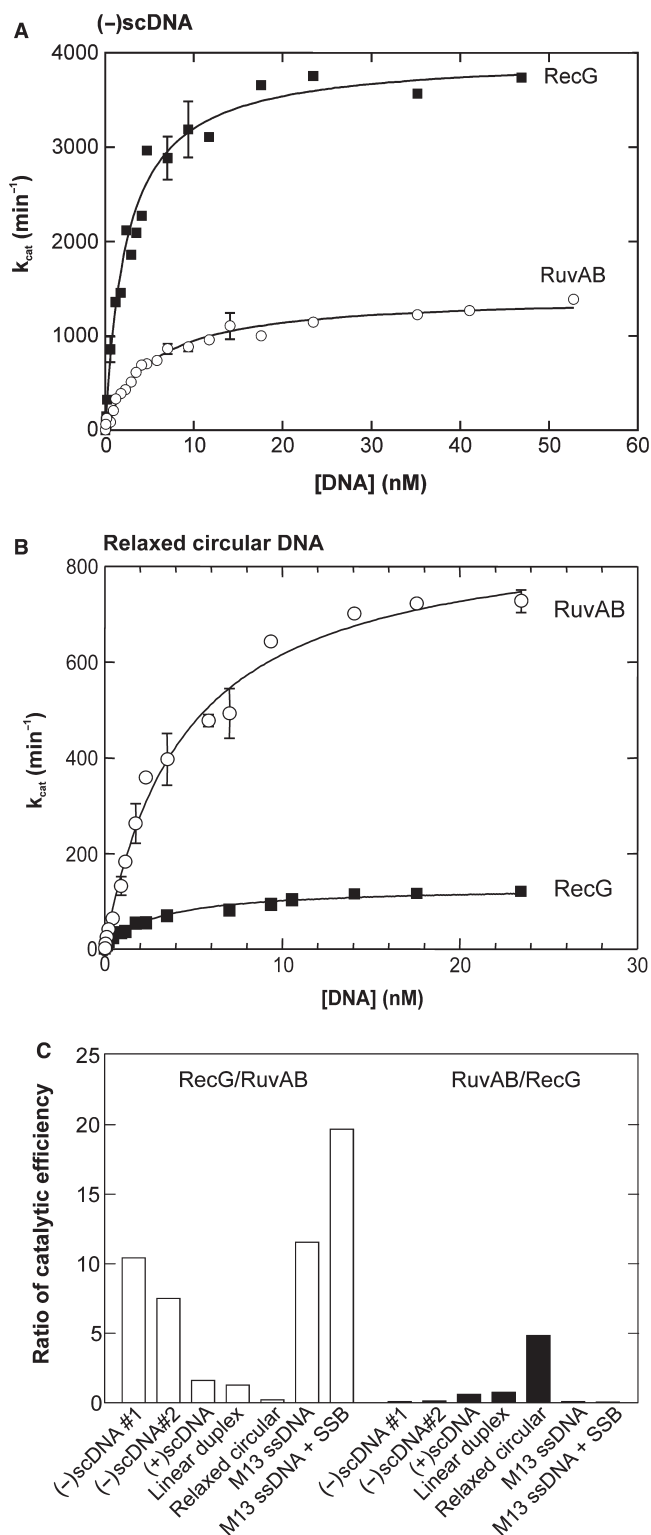
As SSB protein plays an integral role in the interactions of these proteins with ssDNA, its effect on the ATPase activity of each protein was evaluated. Here, a DNA titration was done for each enzyme using a stoichiometric ratio of SSB to M13 ssDNA at each DNA concentration (i.e. the concentration of both was varied.) As observed previously, the presence of SSB results in a stimulation in the ATPase activity of RecG as seen in the 1.6-fold increase in k_{cat} [Table 2 and (44)]. This increase in k_{cat} however is accompanied by a 3.2-fold increase in the apparent K_m^{DNA} so that the resulting catalytic efficiency decreases to $767 \, \text{min}^{-1} \text{nM}^{-1}$ (Table 2). In contrast, the presence of SSB resulted in a significant decrease in the ATPase activity of RuvAB as shown by the 2.4-fold reduction in k_{cat} and a 3.3-fold decrease in catalytic efficiency (Table 2). The apparent affinity of RuvAB for ssDNA was not significantly affected by the presence of SSB protein however. Even though the catalytic efficiency of both enzymes is lower in the presence of SSB, the catalytic efficiency of RecG is still 20-fold higher than that of RuvAB.

(+)scDNA is a poor cofactor for RecG

At the very earliest times following stalling of the replication machinery but prior to replisome disassembly, the DNA may still be positively supercoiled. If the replication machinery dissociates from the fork then the superhelical tension in the DNA can drive the regression of the fork producing a chicken foot structure (12). As RecG binds to (+)scDNA with low affinity (44), it is conceivable that RuvAB may exhibit a strong preference for (+)scDNA and this could be exhibited in a high level of activity in the presence of this DNA cofactor. This may explain why mutations in *ruvAB* have a strong phenotype in the failure to recover following DNA damage (4).

As before, a DNA titration was done and the rates of ATP hydrolysis monitored for each protein in

Table 1. RecG and SSB form a stable complex on ssDNA[a]

Protein(s) Present	DNA present	1st peak elution volume (ml)	2nd peak elution volume (ml)	Proteins present in the 1st peak[b]
None	M13 ssDNA	7.5	NR	None
SSB	None	16.4	NR	SSB
RecG	None	16.4	NR	RecG
RuvB	None	14.5	NR	RuvB
Gp32	None	25	NR	Gp32
SSB	M13 ssDNA	7.1	16	SSB
SSB + RecG	M13 ssDNA	6.5	16.4	SSB + RecG
SSB + RuvB	M13 ssDNA	7.1	15	SSB
Gp32 + RecG	M13 ssDNA	7.5	25	Gp32

[a]The analysis of gel filtration profiles is shown. Data for DNA or protein only are from single runs. Proteins and DNA are from two runs done under similar conditions.
[b]To determine the protein composition of peaks, samples from peak fractions were subjected to electrophoresis in SDS–PAGE gels and stained with Coomassie or silver. To ascertain whether DNA was present in peak fractions, samples were simultaneously subjected to electrophoresis in agarose gels and stained with ethidium bromide (Figure 4).
NR, not relevant.

Table 2. Summary of the kinetic parameters for RecG and RuvAB[a]

DNA cofactor	RecG			RuvAB		
	k_{cat} (min^{-1})	$K_m^{DNA, app}$ (nM)[c]	k_{cat}/K_m (min^{-1}nM^{-1})	k_{cat} (min^{-1})	$K_m^{DNA, app}$ (nM)[c]	k_{cat}/K_m (min^{-1}nM^{-1})
M13 ssDNA[b]	1118 ± 36	0.75 ± 0.07	1491	383 ± 12	2.97 ± 0.14	129
M13 ssDNA + 1:20 SSB[d]	1841 ± 235	2.40 ± 0.80	767	159 ± 23	4.13 ± 0.9	39
(−)scDNA#1	3960 ± 97	2.39 ± 0.22	1657	892 ± 19	5.62 ± 0.38	159
(−)scDNA#2	3200 ± 61	1.92 ± 0.15	1667	844 ± 20	3.80 ± 0.29	222
Linear dsDNA	4960 ± 188	23.3 ± 2.17	213	844 ± 19	5.13 ± 0.41	165
Relaxed circular DNA	140 ± 5	3.37 ± 0.40	41.5	886 ± 3	4.40 ± 0.41	201
(+)scDNA	4010 ± 240	13.43 ± 1.20	299	1017 ± 64	5.50 ± 0.88	185

[a]The values for all parameters were obtained from DNA titrations such as those shown in Figure 4. The values shown are from two separate experiments for each DNA cofactor for each enzyme. The values for k_{cat} and $K_m^{DNA, app}$ were obtained from fitting of the data by the Hill equation and allowing the parameters n, V_{max} and K_m (or $S_{0.5}$) to be fit by the computer.
[b]For all cofactors except M13 ssDNA, the value of n was 1. For RecG the value of n in the presence of M13 ssDNA was 1.41 ± 0.12 and for RuvAB, the value of n was determined to be 2.52 ± 0.29.
[c]$K_m^{DNA, app}$ is reported in nanometer molecules.
[d]A ratio of 1 SSB per 20 nucleotides was used for each DNA concentration in the titration to obtain kinetic parameters. In these experiments, SSB was bound to M13 ssDNA prior to the addition of RecG.

Figure 5. The preferred cofactor for RecG is (−)scDNA whereas for RuvAB it is relaxed circular DNA. (**A**) (−)scDNA and (**B**) relaxed circular DNA. ATPase assays were performed as described in Materials and methods section and were initiated by the addition of protein. The assays for each DNA cofactor were done at the optimal Mg^{+2} concentration for that cofactor as determined previously for RecG or in separate assays for RuvAB [this work and (44,45,49)]. Time courses were analyzed by linear regression to determine reaction rate and the resulting rates are graphed as a function of DNA concentration. RecG was present at 100 nM and

separate experiments. ATPase activity was observed for each protein with a k_{cat} of $4010 \pm 240\,min^{-1}$ being observed for RecG and $1017 \pm 64\,min^{-1}$ for RuvAB (Table 2). Since RecG binds to (+)scDNA with low affinity (the $K_m^{DNA, app}$ is $13.43 \pm 1.2\,nM$), it was not possible to achieve the elevated concentrations of DNA required to accurately determine the apparent K_m^{DNA} in this experiment (i.e. at least 70 nM molecules or $\sim 5 \times K_m$). Therefore, for RecG we can only present values which were determined by extrapolation from the data in the experiments. For RuvAB, we were able to achieve $4 \times K_m$ so that an almost complete data set was obtained. Regardless, the data show that for RecG although the k_{cat} was among the highest of the cofactors used in this study ($4010 \pm 240\,min^{-1}$), the elevated $K_m^{DNA, app}$ was also among the highest ($13.43 \pm 1.20\,nM$; Table 2). This resulted in the catalytic efficiency being poor and comparable to that observed on linear dsDNA (Table 2). In contrast, the k_{cat} for RuvAB in the presence of (+)scDNA is the highest for the DNA cofactors used in this study ($1017 \pm 64\,min^{-1}$; Table 2). However, the resulting catalytic efficiency is comparable to that of the other cofactors used for RuvAB and is 1.6-fold lower than that observed for RecG.

The activity of RecG is higher on (−)scDNA

Our previous characterization of the ATPase activity of RecG revealed a surprisingly strong preference for (−)scDNA (44). To determine whether RuvAB exhibited a similar DNA cofactor preference, separate ATPase assays were done where the concentration of DNA was varied and the rates of ATP hydrolysis determined. As before, RecG exhibits significant ATPase activity in the presence of (−)scDNA with a k_{cat} of $3963 \pm 97\,min^{-1}$ that is 4.7-fold higher than that observed for RuvAB ($851 \pm 19\,min^{-1}$; Figure 5A and Table 2). The higher activity observed for RecG relative to RuvAB is not simply the result of an artifact of the alkaline lysis procedure used to purify the DNA substrate producing structures, such as extruded ssDNA regions that would facilitate loading of either RecG or RuvA. To demonstrate this, experiments were done using (−)scDNA that was purified using a triton lysis procedure (47). Similar results were obtained for both proteins using this (−)scDNA preparation, with RecG exhibiting identical catalytic efficiencies and which are 8- to 10-fold higher than that observed for RuvAB (Table 2).

The activity of RuvAB is higher on relaxed circular DNA

Once (−)scDNA is converted to the relaxed circular form it no longer functions as a cofactor for the ATPase activity of RecG (44). If the model we proposed is correct i.e. once the DNA is relaxed, RecG function can no longer act to regress the DNA at a stalled replication fork, then perhaps RuvAB may function instead. This may be exhibited as a higher level of RuvAB-dependent ATPase activity on relaxed circular DNA relative to that of RecG.

To determine if this could occur, experiments were done using relaxed DNA. As for (−)scDNA, a DNA titration was done under optimal magnesium and ATP concentrations for each protein in the presence of this DNA cofactor. The data show that RuvAB exhibits a 5-fold higher catalytic efficiency than RecG in the presence of this DNA cofactor (Figure 5B and Table 2). It is important to note that the k_{cat} for RuvAB ($886 \pm 3 \, min^{-1}$) remains essentially the same as that on (−)scDNA, while for RecG this decreases ∼26-fold, down from an average of 3580 to $140 \pm 5 \, min^{-1}$.

The apparent affinity for DNA for RecG is cofactor-dependent whereas it is invariant for RuvAB

To begin to understand the underlying reason(s) for the DNA preferences for these enzymes, we examined the catalytic efficiency of each enzyme and compared these as a protein : protein ratio (Figure 5C). When displayed in this manner, it is clear that the substrates which favor the action of RecG are (−)scDNA, ssDNA and SSB-coated ssDNA. In contrast, the only substrate which favors the action of RuvAB is relaxed circular DNA. For (+)scDNA, RecG exhibits a 1.6-fold higher preference. We note however, that the k_{cat} for both enzymes is very high in the presence of (+)scDNA.

Further analysis of the kinetic parameters obtained from each of the DNA titrations for each of the proteins, provides some insight into as to why this might be. A significant factor contributing to the ability of a DNA molecule to function as a cofactor for the hydrolysis of ATP is affinity of the enzyme for that DNA, i.e. the $K_m^{DNA, app}$. Surprisingly, the apparent affinity of RuvAB for each DNA cofactor varies only 1.9-fold ranging from 2.97 ± 0.14 for M13 ssDNA to $5.62 \pm 0.38 \, nM$ for (−)scDNA (Table 2). In sharp contrast, the apparent affinity of RecG for the DNA cofactors varies as much as 29-fold with the highest observed for ssDNA and the lowest for linear duplex DNA (Table 2). Thus the inability of DNA molecules such as (−)scDNA or M13 ssDNA to stimulate the ATPase activity for RuvAB is more complex than a simple change in the apparent affinity for a DNA cofactor (the reason for this is currently unclear). For RecG however, the apparent affinity of the enzyme for DNA is clearly affected by the type or structure of the DNA molecule and is a critical component of the range of DNA molecules on which the enzyme can act.

DISCUSSION

The primary conclusion of this work is that RecG acts first to regress stalled replication forks. This conclusion is derived from data showing a physical interaction between RecG and SSB and from kinetic assays showing that the catalytic efficiency of RecG is higher than that of RuvAB on ssDNA, (−)supercoiled DNA and SSB-coated M13 ssDNA.

The primary conclusion is in agreement with *in vivo* data showing continuous and dynamic association of PriA, RecQ and RecG with active replication forks, an association that is mediated by SSB (61). This dynamic association is consistent with our *in vitro* binding data as well as that of others (54,59). Significantly, it provides a means for rapid association of the correct repair proteins should a fork encounter a blockage: RecG if the fork must be regressed (13,62); PriA to reload DnaB (63); RecQ if the DNA is to be decatenated or otherwise untangled (64,65); RecQ and Topoisomerase III if converging replication forks require resolution (60) and the combination of PriA and RecG to stabilize forks (33,66). For all of these key repair proteins, they are directed to the fork via SSB and this involves a species-specific interaction with the C-terminus of SSB.

The results presented herein are consistent with a model suggesting that DNA topology or structure at a stalled replication fork influences the timing of binding of repair proteins to the DNA (44). Consequently, this will affect the repair pathway taken. If the resulting structures in the vicinity of the fork contain ssDNA, they will be bound by SSB which will direct the loading of RecG (not RuvAB) onto the DNA. Similarly, when superhelical tension is present in the DNA, specifically when the DNA is negatively supercoiled, RecG is favored to act. Additionally, if (+)superhelical tension persists, then there is only a slight preference for RecG as reflected in the higher catalytic efficiency relative to that of RuvAB. Once the DNA has been relaxed, perhaps as a result of the replication machinery dissociating from the DNA leading to protein-independent fork regression or alternatively, following the action of RecG, only then would RuvAB be favored to act (12,29).

The *E. coli* chromosome exists in fluid, topological domains ∼10 kB in size (67). During DNA replication, these domains alter position as the fork moves through the chromosome, with a pre-replicated domain ahead of the replication machinery, a replicating domain in the immediate proximity of the replisome and a replicated domain in the replisome's wake [Figure 6 and (68)]. Consequently, DNA in the pre- and post-replicated domains is (−)supercoiled due to the actions of DNA gyrase and/or topoisomerase IV (69), while DNA within the replicating domain is (+)supercoiled. As the (+) supercoils immediately in front of the fork can equilibrate across the fork to create (+) precatenanes (70), DNA immediately flanking the replisome on both sides is (+) supercoiled. Not surprisingly, during active replication neither RecG nor RuvAB would be expected to be associated with (+)supercoiled DNA in the vicinity of the replication fork. This follows since if the fork is moving, DNA damage is absent and there really is no obvious need for either protein to be associated with the functional replication fork (Figure 6, center panel).
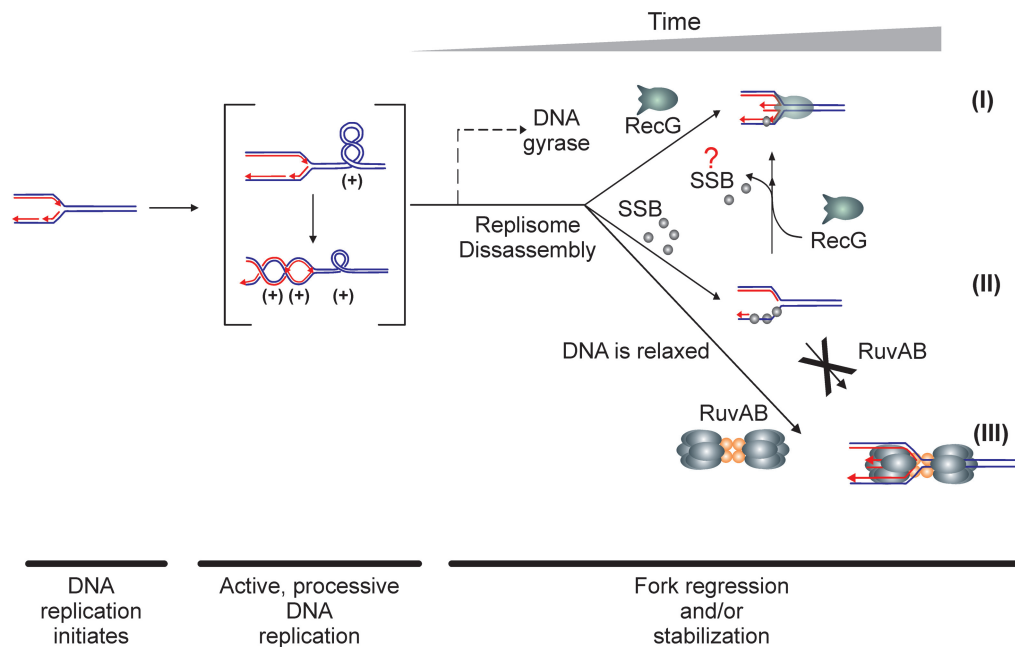
Figure 6. DNA topology influences the timing of protein loading at stalled replication forks. A model of the topological domains of a segment of the *E. coli* chromosome undergoing replication is shown. This figure is adapted from (44). Parental DNA is colored blue and nascent daughter DNA is colored red with arrowheads indicating 3'-ends. Once the fork encounters a block, one of several temporally spaced events may occur. (**I**) If DNA gyrase acts prior to the dissociation of the replication machinery (i.e. within the 5–7 min window following fork stalling), the (+)scDNA is converted to (−)scDNA. RecG binds to the (−)scDNA and drives fork regression. (**II**) If the replisome disassembles exposing a gap in the lagging strand, the gap will be rapidly bound by SSB (grey spheres). RecG binds and together they coexist on ssDNA to stabilize and/or reverse the fork. (**III**) The replication machinery disassembles from the DNA, releasing superhelical tension leading to protein-independent fork regression. The nascent, relaxed DNA is the preferred cofactor for RuvAB.

However, should the fork encounter a translocation block resulting in replisome stalling the situation changes dramatically (Figure 6, right panel). If the replisome disassembles immediately after the block is encountered, the (+)superhelical tension in the vicinity of the fork could be released, driving the formation of a chickenfoot structure in a protein-independent manner (12). The nascent, extruded chickenfoot structure would be an excellent loading site for either RecG or RuvAB (Figure 6, upper scenario) (23,29). As the concentration of RecG has been estimated to be less than 10 copies per cell (71) and the basal levels of RuvA and RuvB are thought to be 700 and 200 copies per cell respectively (18,72), it is reasonable to suggest in this instance, RuvAB would be favored to act. This makes sense as when proteins exhibit similar apparent affinities for a DNA cofactor, the protein present at the higher concentration would be favored to act. (We note however, that a detailed comparison binding study of each enzyme bound to model branched DNAs has yet to be done). Thus, (+)superhelical tension release drives fork regression first, leading to formation of a structure to which RuvAB binds and directs the repair process instead of RecG.

Previous work suggests that the functional half-life of the replication proteins at a stalled fork is 5–7 min (73,74). If during this period of time, the (+)superhelical tension persists, then it is conceivable that RuvAB or RecG may act to regress the fork using a combination of enzymatic action and superhelical tension to drive regression efficiently. However, the catalytic efficiency of RecG in the presence of (+)scDNA, although low relative to (−)scDNA and M13 ssDNA, is still 1.6-fold higher than that of RuvAB. Therefore, if (+)scDNA were to persist then the data suggest there is a slight preference for the action of RecG relative to that of RuvAB. However, we note that in this instance where comparable levels of activity are observed *in vitro*, the concentrations of each protein *in vivo* may play a key role in determining which enzyme directs the repair pathway taken.

However, if DNA gyrase acts to convert the DNA from (+) to (−)supercoiled during the 5–7 min window before the replisome disassembles, then the DNA immediately ahead of the fork will be negatively instead of positively supercoiled (73,74). As RecG binds to (−)scDNA with high affinity and is the more catalytically efficient enzyme in the presence of this cofactor (i.e. 16-fold higher than RuvAB), DNA in this conformation would be an excellent loading site for RecG (Figure 6, scenario I). The activity we observe for RuvAB in the presence of (−)scDNA is significantly lower than that observed previously (39). We have gone to great lengths to ensure that our scDNA preparations are (−)supercoiled, are free from all contaminating DNA or RNA species and do not contain alkali-induced loops or other regions that can facilitate protein loading (44). Thus we propose that the large difference in activity between RecG and RuvAB in the presence of

(−)scDNA is real and that stalled forks with (−)superhelical tension would be acted upon by RecG only. As (−)scDNA can extrude a chickenfoot structure similar to that observed for (+)scDNA (75), and as RecG can drive fork regression when DNA is (−)supercoiled, these properties could combine to provide an efficient fork regression reaction driven by RecG as shown previously (62).

If replisome stalling leads to a structure with single-stranded DNA gaps in either the leading or lagging strands, the ssDNA within the gap would most likely be bound by SSB (Figure 6, scenario II). This constitutes a favorable situation for RecG since it exhibits significant activity on ssDNA in the absence of SSB protein becoming stabilized in its presence (44). Further, a clear protein–protein interaction between RecG and SSB with a stoichiometry of 2 RecG monomers per SSB tetramer was observed in coprecipitation experiments (Figure 2). Since the interaction is mediated via the C-terminus of SSB, a straightforward interpretation of these data is that each of the RecG monomers interacts with a single C-terminal tail and that due to molecular crowding, binding of additional RecG monomers is prevented. The stoichiometry changed from 2 RecGs per tetramer in solution to 1 RecG per SSB monomer in the presence of ssDNA. The 1:1 stoichiometry most likely reflects a combination of RecG binding to SSB tetramers as well as additional and direct binding of RecG to the ssDNA substrate. In contrast, the catalytic efficiency of RuvAB that we observe on ssDNA is low, consistent with previous work (39,45), ATPase activity is reduced by stoichiometric amounts of SSB relative to ssDNA, RuvAB translocation on ssDNA is inhibited by saturating amounts of SSB protein (40) and neither RuvA, RuvB nor RuvAB interacts with SSB (this work). Finally the catalytic efficiency of RecG is 20-fold higher than that of RuvAB on SSB-coated ssDNA (Figure 4C) and, RecG is catalytically efficient on model forks with either leading or lagging strand gaps (44). Thus, if the stalled fork DNA is single-stranded in character, the data suggest that RecG would be preferentially loaded onto the DNA in a reaction mediated by SSB protein, leading to regression of the fork.

Genetic data have been used to illuminate roles of RecG and RuvAB in DNA repair. The data show that these proteins have overlapping functions with the phenotype of *ruv* mutations being more severe than that of *recG* (7,43). The greater severity of ruv mutations has also been used to argue that RecG plays little or no role in fork reversal and that the primary player is instead RuvAB (4). The data presented in this work show that this is not necessarily correct and that the structure of the DNA at the fork plays a key role in influencing the timing of loading of RecG and RuvAB onto the DNA to direct the repair pathway taken. Further, the data also suggest, but by no means prove, that a key structure that forms must be acted upon by RuvAB, consistent with the severity of the *ruv* phenotype. However, this structure (possibly a Holliday Junction) forms 'late' in the regression pathway following replication fork stalling and can result from a number of processes acting either independently or in concert. This structure can form as a result of RecG action to regress a stalled fork (13). If RecG is absent, alternate mechanisms exist to reverse forks so that repair can be facilitated, including fork regression driven by (+) or (−)superhelical tension independent of enzyme action, or by combinations of protein action and DNA topology. The end result is a DNA structure which is relaxed in nature and possibly resembles a Holliday Junction to which RuvAB binds with high affinity and can process efficiently [Figure 6, scenario III and (4,29,76,77)].

REFERENCES

1. Kogoma,T. (1997) Stable DNA replication: interplay between DNA replication, homologous recombination, and transcription. *Microbiol. Mol. Biol. Rev.*, **61**, 212–238.
2. Kuzminov,A. (1999) Recombinational repair of DNA damage in Escherichia coli and bacteriophage lambda. *Microbiol. Mol. Biol. Rev.*, **63**, 751–813.
3. Kowalczykowski,S.C. (2000) Initiation of genetic recombination and recombination-dependent replication. *Trends Biochem. Sci.*, **25**, 156–165.
4. Seigneur,M., Bidnenko,V., Ehrlich,S.D. and Michel,B. (1998) RuvAB acts at arrested replication forks. *Cell*, **95**, 419–430.
5. Cox,M.M., Goodman,M.F., Kreuzer,K.N., Sherratt,D.J., Sandler,S.J. and Marians,K.J. (2000) The importance of repairing stalled replication forks. *Nature*, **404**, 37–41.
6. Cox,M.M. (2001) Recombinational DNA repair of damaged replication forks in Escherichia coli: questions. *Annu. Rev. Genet.*, **35**, 53–82.
7. McGlynn,P. and Lloyd,R.G. (2002) Genome stability and the processing of damaged replication forks by RecG. *Trends Genet.*, **18**, 413–419.
8. Marians,K.J. (2004) Mechanisms of replication fork restart in Escherichia coli. *Philos. Trans. R. Soc. Lond., B, Biol. Sci.*, **359**, 71–77.
9. Michel,B., Grompone,G., Flores,M.J. and Bidnenko,V. (2004) Multiple pathways process stalled replication forks. *Proc. Natl Acad. Sci. USA*, **101**, 12783–12788.
10. Marians,K.J. (2000) Replication and recombination intersect. *Curr. Opin. Genet. Dev.*, **10**, 151–156.
11. Lusetti,S.L. and Cox,M.M. (2002) The bacterial RecA protein and the recombinational DNA repair of stalled replication forks. *Annu. Rev. Biochem.*, **71**, 71–100.
12. Postow,L., Ullsperger,C., Keller,R.W., Bustamante,C., Vologodskii,A.V. and Cozzarelli,N.R. (2001) Positive torsional strain causes the formation of a four-way junction at replication forks. *J. Biol. Chem.*, **276**, 2790–2796.
13. McGlynn,P. and Lloyd,R.G. (2001) Rescue of stalled replication forks by RecG: simultaneous translocation on the leading and lagging strand templates supports an active DNA unwinding model of fork reversal and Holliday junction formation. *Proc. Natl Acad. Sci. USA*, **98**, 8227–8234.
14. Robu,M.E., Inman,R.B. and Cox,M.M. (2004) Situational repair of replication forks: roles of RecG and RecA proteins. *J. Biol. Chem.*, **279**, 10973–10981.

15. Robu,M.E., Inman,R.B. and Cox,M.M. (2001) RecA protein promotes the regression of stalled replication forks in vitro. *Proc. Natl Acad. Sci. USA*, **98**, 8211–8218.
16. McGlynn,P. and Lloyd,R.G. (2000) Modulation of RNA polymerase by (p)ppGpp reveals a RecG-dependent mechanism for replication fork progression. *Cell*, **101**, 35–45.
17. Lloyd,R.G. and Buckman,C. (1991) Genetic analysis of the recG locus of Escherichia coli K-12 and of its role in recombination and DNA repair. *J. Bacteriol.*, **173**, 1004–1011.
18. West,S.C. (1997) Processing of recombination intermediates by the RuvABC proteins. *Annu. Rev. Genet.*, **31**, 213–244.
19. West,S.C. and Connolly,B. (1992) Biological roles of the Escherichia coli RuvA, RuvB and RuvC proteins revealed. *Mol. Microbiol.*, **6**, 2755–2759.
20. Kowalczykowski,S.C., Dixon,D.A., Eggleston,A.K., Lauder,S.D. and Rehrauer,W.M. (1994) Biochemistry of homologous recombination in Escherichia coli. *Microbiol. Rev.*, **58**, 401–465.
21. Meddows,T.R., Savory,A.P. and Lloyd,R.G. (2004) RecG helicase promotes DNA double-strand break repair. *Mol. Microbiol.*, **52**, 119–132.
22. Jaktaji,R.P. and Lloyd,R.G. (2003) PriA supports two distinct pathways for replication restart in UV-irradiated Escherichia coli cells. *Mol. Microbiol.*, **47**, 1091–1100.
23. McGlynn,P. and Lloyd,R.G. (1999) RecG helicase activity at three- and four-strand DNA structures. *Nucleic Acids Res.*, **27**, 3049–3056.
24. Iwasaki,H., Takahagi,M., Nakata,A. and Shinagawa,H. (1992) Escherichia coli RuvA and RuvB proteins specifically interact with Holliday junctions and promote branch migration. *Genes Dev.*, **6**, 2214–2220.
25. Parsons,C.A., Tsaneva,I., Lloyd,R.G. and West,S.C. (1992) Interaction of Escherichia coli RuvA and RuvB proteins with synthetic Holliday junctions. *Proc. Natl Acad. Sci. USA*, **89**, 5452–5456.
26. Tsaneva,I.R., Muller,B. and West,S.C. (1992) ATP-dependent branch migration of Holliday junctions promoted by the RuvA and RuvB proteins of E. *coli. Cell*, **69**, 1171–1180.
27. Tsaneva,I.R., Illing,G., Lloyd,R.G. and West,S.C. (1992) Purification and properties of the RuvA and RuvB proteins of Escherichia coli. *Mol. Gen. Genet.*, **235**, 1–10.
28. Muller,B. and West,S.C. (1994) Processing of Holliday junctions by the Escherichia coli RuvA, RuvB, RuvC and RecG proteins. *Experientia*, **50**, 216–222.
29. McGlynn,P. and Lloyd,R.G. (2001) Action of RuvAB at replication fork structures. *J. Biol. Chem.*, **276**, 41938–41944.
30. McGlynn,P., Mahdi,A.A. and Lloyd,R.G. (2000) Characterisation of the catalytically active form of RecG helicase. *Nucleic Acids Res.*, **28**, 2324–2332.
31. Singleton,M.R., Scaife,S. and Wigley,D.B. (2001) Structural analysis of DNA replication fork reversal by RecG. *Cell*, **107**, 79–89.
32. Whitby,M.C. and Lloyd,R.G. (1998) Targeting Holliday junctions by the RecG branch migration protein of Escherichia coli. *J. Biol. Chem.*, **273**, 19729–19739.
33. Gregg,A.V., McGlynn,P., Jaktaji,R.P. and Lloyd,R.G. (2002) Direct rescue of stalled DNA replication forks via the combined action of PriA and RecG helicase activities. *Mol. Cell*, **9**, 241–251.
34. Briggs,G.S., Mahdi,A.A., Weller,G.R., Wen,Q. and Lloyd,R.G. (2004) Interplay between DNA replication, recombination and repair based on the structure of RecG helicase. *Philos. Trans. R. Soc. Lond., B, Biol. Sci.*, **359**, 49–59.
35. Sharples,G.J., Benson,F.E., Illing,G.T. and Lloyd,R.G. (1990) Molecular and functional analysis of the ruv region of Escherichia coli K-12 reveals three genes involved in DNA repair and recombination. *Mol. Gen. Genet.*, **221**, 219–226.
36. Rafferty,J.B., Sedelnikova,S.E., Hargreaves,D., Artymiuk,P.J., Baker,P.J., Sharples,G.J., Mahdi,A.A., Lloyd,R.G. and Rice,D.W. (1996) Crystal structure of DNA recombination protein RuvA and a model for its binding to the Holliday junction. *Science*, **274**, 415–421.
37. Hargreaves,D., Rice,D.W., Sedelnikova,S.E., Artymiuk,P.J., Lloyd,R.G. and Rafferty,J.B. (1998) Crystal structure of E.coli RuvA with bound DNA Holliday junction at 6 Å resolution. *Nat. Struct. Biol.*, **5**, 441–446.
38. Muller,B., Tsaneva,I.R. and West,S.C. (1993) Branch migration of Holliday junctions promoted by the Escherichia coli RuvA and RuvB proteins. I. Comparison of RuvAB- and RuvB-mediated reactions. *J. Biol. Chem.*, **268**, 17179–17184.
39. Muller,B., Tsaneva,I.R. and West,S.C. (1993) Branch migration of Holliday junctions promoted by the Escherichia coli RuvA and RuvB proteins. II. Interaction of RuvB with DNA. *J. Biol. Chem.*, **268**, 17185–17189.
40. Tsaneva,I.R., Muller,B. and West,S.C. (1993) RuvA and RuvB proteins of Escherichia coli exhibit DNA helicase activity in vitro. *Proc. Natl Acad. Sci. USA*, **90**, 1315–1319.
41. Dunderdale,H.J., Sharples,G.J., Lloyd,R.G. and West,S.C. (1994) Cloning, overexpression, purification, and characterization of the Escherichia coli RuvC Holliday junction resolvase. *J. Biol. Chem.*, **269**, 5187–5194.
42. Bennett,R.J. and West,S.C. (1996) Resolution of Holliday junctions in genetic recombination: RuvC protein nicks DNA at the point of strand exchange. *Proc. Natl Acad. Sci. USA*, **93**, 12217–12222.
43. Sharples,G.J., Ingleston,S.M. and Lloyd,R.G. (1999) Holliday junction processing in bacteria: insights from the evolutionary conservation of RuvABC, RecG, and RusA. *J. Bacteriol.*, **181**, 5543–5550.
44. Slocum,S.L., Buss,J.A., Kimura,Y. and Bianco,P.R. (2007) Characterization of the ATPase activity of the Escherichia coli RecG protein reveals that the preferred cofactor is negatively supercoiled DNA. *J. Mol. Biol.*, **367**, 647–664.
45. Marrione,P.E. and Cox,M.M. (1996) Allosteric effects of RuvA protein, ATP, and DNA on RuvB protein-mediated ATP hydrolysis. *Biochemistry*, **35**, 11228–11238.
46. Sambrook,J., Fritsch,E.F. and Maniatis,T. (1989) *Molecular Cloning: A Laboratory Manual*, 2nd edn., Cold Spring Harbor Laboratory Press, Cold Spring Harbor, NY.
47. Heller,R.C. and Marians,K.J. (2005) The disposition of nascent strands at stalled replication forks dictates the pathway of replisome loading during restart. *Mol. Cell*, **17**, 733–743.
48. Gill,S.C. and von Hippel,P.H. (1989) Calculation of protein extinction coefficients from amino acid sequence data. *Anal. Biochem.*, **182**, 319–326.
49. Marrione,P.E. and Cox,M.M. (1995) RuvB protein-mediated ATP hydrolysis: functional asymmetry in the RuvB hexamer. *Biochemistry*, **34**, 9809–9818.
50. Lohman,T.M., Green,J.M. and Beyer,R.S. (1986) Large-scale overproduction and rapid purification of the Escherichia coli ssb gene product. Expression of the ssb gene under lambda P_L control. *Biochemistry*, **25**, 21–25.
51. Lohman,T.M. and Overman,L.B. (1985) Two binding modes in Escherichia coli single strand binding protein-single stranded DNA complexes. Modulation by NaCl concentration. *J. Biol. Chem.*, **260**, 3594–3603.
52. Bianco,P.R. and Hurley,E.M. (2005) The type I restriction endonuclease EcoR124I, couples ATP hydrolysis to bidirectional DNA translocation. *J. Mol. Biol.*, **352**, 837–859.
53. Kelly,R.C., Jensen,D.E. and von Hippel,P.H. (1976) DNA ''melting'' proteins. IV. Fluorescence measurements of binding parameters for bacteriophage T4 gene 32-protein to mono-, oligo-, and polynucleotides. *J. Biol. Chem.*, **251**, 7240–7250.
54. Shereda,R.D., Bernstein,D.A. and Keck,J.L. (2007) A central role for SSB in Escherichia coli RecQ DNA helicase function. *J. Biol. Chem.*, **282**, 19247–19258.
55. Savvides,S.N., Raghunathan,S., Futterer,K., Kozlov,A.G., Lohman,T.M. and Waksman,G. (2004) The C-terminal domain of full-length E. coli SSB is disordered even when bound to DNA. *Protein Sci.*, **13**, 1942–1947.
56. Genschel,J., Curth,U. and Urbanke,C. (2000) Interaction of E. coli single-stranded DNA binding protein (SSB) with exonuclease I. The carboxy-terminus of SSB is the recognition site for the nuclease. *Biol. Chem.*, **381**, 183–192.
57. Handa,P., Acharya,N. and Varshney,U. (2001) Chimeras between single-stranded DNA-binding proteins from Escherichia coli and Mycobacterium tuberculosis reveal that their C-terminal domains interact with uracil DNA glycosylases. *J. Biol. Chem.*, **276**, 16992–16997.
58. Witte,G., Urbanke,C. and Curth,U. (2003) DNA polymerase III chi subunit ties single-stranded DNA binding protein to the bacterial replication machinery. *Nucleic Acids Res.*, **31**, 4434–4440.

59. Cadman,C.J. and McGlynn,P. (2004) PriA helicase and SSB interact physically and functionally. *Nucleic Acids Res.*, **32**, 6378–6387.

60. Suski,C. and Marians,K.J. (2008) Resolution of converging replication forks by RecQ and topoisomerase III. *Mol. Cell*, **30**, 779–789.

61. Lecointe,F., Serena,C., Velten,M., Costes,A., McGovern,S., Meile,J.C., Errington,J., Ehrlich,S.D., Noirot,P. and Polard,P. (2007) Anticipating chromosomal replication fork arrest: SSB targets repair DNA helicases to active forks. *EMBO J.*, **26**, 4239–4251.

62. McGlynn,P., Lloyd,R.G. and Marians,K.J. (2001) Formation of Holliday junctions by regression of nascent DNA in intermediates containing stalled replication forks: RecG stimulates regression even when the DNA is negatively supercoiled. *Proc. Natl Acad. Sci. USA*, **98**, 8235–8240.

63. Marians,K.J. (1999) PriA: at the crossroads of DNA replication and recombination. *Prog. Nucleic Acid Res. Mol. Biol.*, **63**, 39–67.

64. Harmon,F.G., Brockman,J.P. and Kowalczykowski,S.C. (2003) RecQ helicase stimulates both DNA catenation and changes in DNA topology by topoisomerase III. *J. Biol. Chem.*, **278**, 42668–42678.

65. Harmon,F.G. and Kowalczykowski,S.C. (1998) RecQ helicase, in concert with RecA and SSB proteins, initiates and disrupts DNA recombination. *Genes Dev.*, **12**, 1134–1144.

66. Tanaka,T. and Masai,H. (2006) Stabilization of a stalled replication fork by concerted actions of two helicases. *J. Biol. Chem.*, **281**, 3484–3493.

67. Postow,L., Hardy,C.D., Arsuaga,J. and Cozzarelli,N.R. (2004) Topological domain structure of the Escherichia coli chromosome. *Genes Dev.*, **18**, 1766–1779.

68. Postow,L., Crisona,N.J., Peter,B.J., Hardy,C.D. and Cozzarelli,N.R. (2001) Topological challenges to DNA replication: conformations at the fork. *Proc. Natl Acad. Sci. USA*, **98**, 8219–8226.

69. Hiasa,H. and Marians,K.J. (1994) Topoisomerase IV can support oriC DNA replication in vitro. *J. Biol. Chem.*, **269**, 16371–16375.

70. Peter,B.J., Ullsperger,C., Hiasa,H., Marians,K.J. and Cozzarelli,N.R. (1998) The structure of supercoiled intermediates in DNA replication. *Cell*, **94**, 819–827.

71. Lloyd,R.G. and Sharples,G.J. (1991) Molecular organization and nucleotide sequence of the recG locus of Escherichia coli K-12. *J. Bacteriol.*, **173**, 6837–6843.

72. Shurvinton,C.E. and Lloyd,R.G. (1982) Damage to DNA induces expression of the ruv gene of Escherichia coli. *Mol. Gen. Genet.*, **185**, 352–355.

73. Marians,K.J., Hiasa,H., Kim,D.R. and McHenry,C.S. (1998) Role of the core DNA polymerase III subunits at the replication fork. Alpha is the only subunit required for processive replication. *J. Biol. Chem.*, **273**, 2452–2457.

74. McGlynn,P. and Guy,C.P. (2008) Replication forks blocked by protein-DNA complexes have limited stability in vitro. *J. Mol. Biol.*, **381**, 249–255.

75. Lilley,D.M. (1980) The inverted repeat as a recognizable structural feature in supercoiled DNA molecules. *Proc. Natl Acad. Sci. USA*, **77**, 6468–6472.

76. Flores,M.J., Bierne,H., Ehrlich,S.D. and Michel,B. (2001) Impairment of lagging strand synthesis triggers the formation of a RuvABC substrate at replication forks. *EMBO J.*, **20**, 619–629.

77. Seigneur,M., Ehrlich,S.D. and Michel,B. (2000) RuvABC-dependent double-strand breaks in dnaBts mutants require recA. *Mol. Microbiol.*, **38**, 565–574.

78. Segel,I.H. (1976) *Biochemical Calculations*, 2nd edn., John Wiley and Sons, Hoboken, NJ, USA.